

***GPX2* and *BMP4* as Significant Molecular Alterations in The Lung Adenocarcinoma Progression: Integrated Bioinformatics Analysis**

Mohammad Hossein Derakhshan Nazari, B.Sc.^{1#}, Rana Askari Dastjerdi, B.Sc.^{1#}, Parnian Ghaedi Talkhouncheh, B.Sc.^{2#}, Ahmad Bereimipour, M.Sc.³, Hamidreza Mollasalehi, Ph.D.², Amir Ali Mahshad, B.Sc.¹, Ali Razi, B.Sc.⁴, Mohammad Hossein Nazari, M.Sc.⁵, Amin Ebrahimi Sadrabadi, Ph.D.^{3*}, Sara Taleahmad, Ph.D.^{3*}

1. Department of Microbiology and Microbial Biotechnology, Faculty of Life Science and Biotechnology, Shahid Beheshti University, Tehran, Iran
2. Department of Cell and Molecular Biology, Faculty of Life Science and Biotechnology, Shahid Beheshti University, Tehran, Iran
3. Department of Stem Cells and Developmental Biology, Cell Science Research Center, Royan Institute for Stem Cell Biology and Technology, ACECR, Tehran, Iran
4. Biophysics Department, Science Faculty, York University, Toronto, Canada
5. V. Zelman Institute for Medicine and Psychology, Novosibirsk State University, Novosibirsk, Russia

*Corresponding Address: P.O. Box: 16635-148, Department of Stem Cells and Developmental Biology, Cell Science Research Center, Royan Institute for Stem Cell Biology and Technology, ACECR, Tehran, Iran

Emails: amin.ebrahimi@royaninstitute.org, s.taleahmad@royan-rc.ac.ir

#These authors contributed equally to this work.

Received: 06/January/2021, Accepted: 19/April/2021

Abstract

Objectives: Non-small cell lung adenocarcinoma (NSCLC) is the most common type of lung cancer, which is considered as the most lethal and prevalent cancer worldwide. Recently, molecular changes have been implicated to play a significant role in the cancer progression. Despite of numerous studies, the molecular mechanism of NSCLC pathogenesis in each sub-stage remains unclear. Studying these molecular alterations gives us a chance to design successful therapeutic plans which is aimed in this research.

Materials and Methods: In this bioinformatics study, we compared the expression profile of 7 minor stages of NSCLC adenocarcinoma, including GSE41271, GSE42127, and GSE75037, to clarify the relation of molecular alterations and tumorigenesis. At first, 99 common differentially expressed genes (DEG) were obtained. Then, functional enrichment analysis and protein-protein interaction (PPI) network construction were performed to uncover the association of significant cellular and molecular changes. Finally, gene expression profile interactive analysis (GEPIA) was employed to validate the results by RNA-seq expression data.

Results: Primary analysis showed that *BMP4* was downregulated through the tumor progression to the stage IB and *GPX2* was upregulated in the course of final tumor development to the stage IV and distant metastasis. Functional enrichment analysis indicated that *BMP4* in the TGF- β signaling pathway and *GPX2* in the glutathione metabolism pathway may be the key genes for NSCLC adenocarcinoma progression. GEPIA analysis revealed a correlation between *BMP4* downregulation and *GPX2* upregulation and lung adenocarcinoma (LUAD) progression and lower survival chances in LUAD patients which confirm microarray data.

Conclusion: Taken together, we suggested *GPX2* as an oncogene by inhibiting apoptosis, promoting EMT and increasing glucose uptake in the final stages and *BMP4* as a tumor suppressor via inducing apoptosis and arresting cell cycle in the early stages through lung adenocarcinoma (ADC) development to make them candidate genes to further cancer therapy investigations.

Keywords: Glutathione Peroxidase, In Silico, Microarray, NSCLC, TGF- β Signaling

Cell Journal (Yakhteh), Vol 24, No 6, June 2022, Pages: 302-308

Citation: Derakhshan Nazari MH, Askari Dastjerdi R, Ghaedi Talkhouncheh P, Bereimipour A, Mollasalehi H, Mahshad AA, Razi A, Nazari MH, Ebrahimi Sadrabadi A, Taleahmad S. *GPX2* and *BMP4* as significant molecular alterations in the lung adenocarcinoma progression: integrated bioinformatics analysis. Cell J. 2022; 24(6): 302-308. doi: 10.22074/cellj.2022.7930.

This open-access article has been published under the terms of the Creative Commons Attribution Non-Commercial 3.0 (CC BY-NC 3.0).

Introduction

Lung cancer is the leading cause of cancer-related death worldwide. In 2012, approximately 1.8 million cases were diagnosed, and 1.6 million died from lung cancer (1). Besides, 2,093,876 new cases and 1,761,007 deaths were confirmed in 2018, accounting for 18.4 percent of cancer deaths (2). Two main reasons are considered to contribute to the high incidence and mortality of lung cancer. The

smoking habit is believed the first reason, because 80 to 90% of diagnosed patients have been reported with a history of smoking (3, 4). And the second one stems from poor diagnosis. Roughly 70% of patients have been diagnosed with locally advanced or metastatic tumors (5). Except for current smoking, some other risk factors such as passive or second-hand smoking, diet, air pollution, alcohol, physical activity, occupational exposure, and genetic

factors have been introduced to have a role in lung cancer progression (5, 6). Lung cancer has two main subtypes: Non-small cell lung cancer (NSCLC) and small cell lung cancer (SCLC) (7). NSCLC makes up approximately 83% of lung cancers (8) and is divided into three main histological subtypes, including squamous cell carcinoma (SCC), large cell carcinoma (LCC), and adenocarcinoma (ADC). NSCLC adenocarcinoma has shown with a higher incidence of NSCLC cases (50%) (9). NSCLC staging, like many cancers, is based on the tumor, nodes and metastasis (TNM) staging system (10) that T stands for the pathological extension of tumor size, N describes the involvement of regional lymph nodes, and M shows distant metastasis (11). Tumor progression, according to the TNM, starts from sub-stage IA (stage I) and end up to stage IV. However, there is a stage 0 called carcinoma in situ (CIS) before sub-stage IA that is usually medicated by an accurate resection. It has been estimated that 5-year survival in NSLCC varies from 73% in stage IA patients to 13% in stage IV patients (12). Selecting a therapeutic method for NSCLC is based on the tumor stage recommending resection for stage I, resection, and adjuvant chemotherapy for stage II, chemotherapy, and radiotherapy for stage III and chemotherapy platinum-based two drugs for stage IV (4, 5). However, recently, targeting molecular events in cancer cells has been implicated as a novel method for cancer therapy (13).

In the process of tumor progression, many genetic alterations can occur, and some researches have been accomplished to elucidate these molecular changes in the NSCLC ADC to treat and prevent cancer progression, but it remains unclear. Genetic alterations, especially expression changes, mediate many biological programs to provide an appropriate statue for malignant cell's rapid proliferation (14). Conclusively, the identification of molecular signature alterations impacting tumor progression that is aimed in this study could be helpful for more investigations for treatment, prognosis, and diagnosis of NSCLC adenocarcinoma.

High-throughput methods such as microarrays have been used for bioinformatics analysis and provided useful information for monitoring biomarkers and discernment of the pathogenic genes in cancer and other diseases that are fundamental for therapeutic targets (15, 16). In this study, we analyzed microarray expression profiles of 3 cohorts with GEO2R based on the R language. Subsequently, functional annotations analysis was performed to uncover the association between molecular alterations and neoplastic cell proliferation.

Materials and Methods

Microarray data analysis

In this bioinformatics study, gene expression profiles of GSE75037, GSE41271, and GSE42127 were extracted from the GEO (<https://www.ncbi.nlm.nih.gov/geo/>) containing 179, 132, and 82 chips for adenocarcinoma, and then 28, 25, and 22 chips were selected respectively. Gene expression profiles in these series were examined

based on the GPL6884 Platform (Illumina Human WG-6V3.0 Expression Bead Chip). ADC samples with the highest similarity in the value distribution in 7 different sub-stages (according to the TNM staging) (11, 12) were divided into six groups in order to screen the molecular alterations in tumor progression (from stage IA to IV) and were subsequently analyzed by GEO2R (Table S1, See Supplementary Online Information at www.celljournal.org). Twelve samples were chosen for stages IIIA, IIB, IB, and IA, and 11, 9, and 7 samples were selected for stage IIA, IIIB, and IV, respectively. Then, comparison of the gene expression profile of stages was performed in 6 groups (Table 1). Using GEO2R, differentially expressed genes (DEGs) were identified in each group with the criterion cut-off $P < 0.05$ and $|\text{LogFC}| \geq 1$ for statistical significance. Then the DEGs were shared in each group in three data series using the Venn diagram to identify the most predominant molecular alterations. A heatmap was then designed by a web-based tool, Morpheus (<https://software.broadinstitute.org/morpheus/>), to screen dysregulated genes expression level.

Table 1: Stages samples in each groups

Groups	Stage comparison	Samples count
Group 1	IA vs. IB	12 vs. 12
Group 2	IB vs. IIA	12 vs. 11
Group 3	IIA vs. IIB	11 vs. 12
Group 4	IIB vs. IIIA	12 vs. 12
Group 5	IIIA vs. IIIB	12 vs. 9
Group 6	IIIB vs. IV	9 vs. 7

Functional annotation analysis

Gene ontology (GO) and pathway enrichment analysis were performed using GO Resource (GOR, <http://geneontology.org/>), Kyoto Encyclopedia of Genes and Genomes (KEGG, <https://www.genome.jp/kegg/pathway.html>), Database for Annotation, Visualization and Integrated Discovery (DAVID, <https://david.ncifcrf.gov/>), Wikipathways (<https://wikipathways.org/>), Reactome (<https://reactome.org/>) and BioPlanet (<https://tripod.nih.gov/bioplanet/>). The statistically significant pathways and GOs were defined by $P < 0.05$ as the cut-off criterion. Then protein-protein interaction (PPI) network was constructed using the Search Tool for the Retrieval of Interacting Genes (STRING, <https://string-db.org/>) (17) and a combined score > 0.4 was used to identify significant interactions. Next, Cytoscape (version 3.8.0) was used with CentiScape2.2 and CytoHubba plugins to discover hub proteins and visualization of the PPI network.

Candidate genes analysis by GEPIA

GEPIA (<http://gepia.cancer-pku.cn/>) as a newly developed interactive web server for analyzing the RNA sequencing

expression data using TCGA (<https://www.cancer.gov/about-nci/organization/ccg/research/structural-genomics/tcga>) and GTEx (<https://gtexportal.org/home/>) projects was applied for additional analysis of candidate genes in lung adenocarcinoma (LUAD) and comparison with squamous cell carcinoma (LUSC) with the $|\text{LogFC}| \geq 1$ and $P < 0.01$ as the cut-off criterion. Finally, Kaplan-Meier plot matched to the TCGA data was used to explain the survival rate of patients, according to the expression of candidate genes in GEPIA database.

Results

Identification of differentially expressed genes

A total of 16786 DEGs was identified in the NSCLC adenocarcinoma expression datasets GSE41271, GSE42127, and GSE75037 using GEO2R. Ninety-nine common DEGs in all groups (Table S2, See Supplementary Online Information at www.celljournal.org), including 58 downregulated and 41 upregulated DEGs, were obtained through the Venn diagram (Fig. 1A). The group 1 (stage IA vs. stage IB) included most DEGs with 40 downregulated and 29 upregulated genes, indicating that the most molecular alterations have occurred in the early stages. A heatmap of up (blue) and downregulated (red) genes visualized between three different studies (Fig. 1B). Top DEGs $|\text{LogFC}| \geq 2$ between 6 groups are shown in the Table S3 (See Supplementary Online Information at www.celljournal.org). Eventually, our analysis represented *ITLN2*, *CLDN10*, *SLC7A2*, *GFR43*, and *GPX2* as the most altered genes in the groups 1 to 6, respectively, and among these genes, *GPX2* was the most altered gene with a noticeable 43.56-fold change.

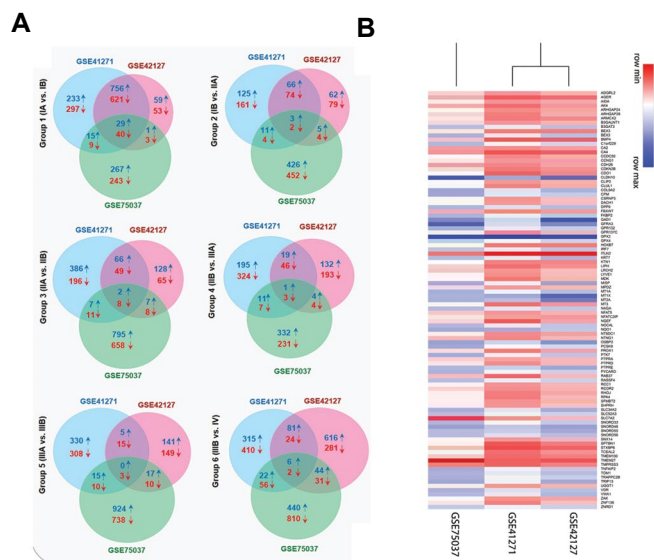


Fig.1: Intersecting genes of GSE41271, GSE42127, and GSE75037 in each sub-stage using a Venn diagram. **A.** Overlapping genes in GSE41271, GSE42127, and GSE75037 in group 1 (IA vs. IB), group 2 (IB vs. IIA), group 3 (IIA vs. IIB), group 4 (IIB vs. IIIA), group 5 (IIIA vs. IIIB), and group 6 (IIIB vs. IV) via Venn diagram ↓ indicates downregulated and ↑ indicates upregulated differentially expressed genes (DEG) respectively. Red numbers refer to downregulated common DEGs and blue numbers are related to the upregulated common DEGs. **B.** A heatmap of differentially expressed genes between three studies. Each row of the heatmap represents a gene that has at least a $|\text{LogFC}| \geq 1$ between three studies. Red for lower and blue for higher expressions.

Discovering associated gene ontology and pathways

GO was analyzed by Enrichr and DAVID in order to find out enriched BP, MF, and CC. In this manner, for downregulated DEGs smooth muscle tissue development, carbonate dehydratase activity, and endoplasmic reticulum-Golgi intermediate compartment were manifested. Then for upregulated DEGs, cellular response to zinc ion, cysteine-type endopeptidase activator activity involved in the apoptotic process and perinuclear region of cytoplasm were revealed (Fig.2).

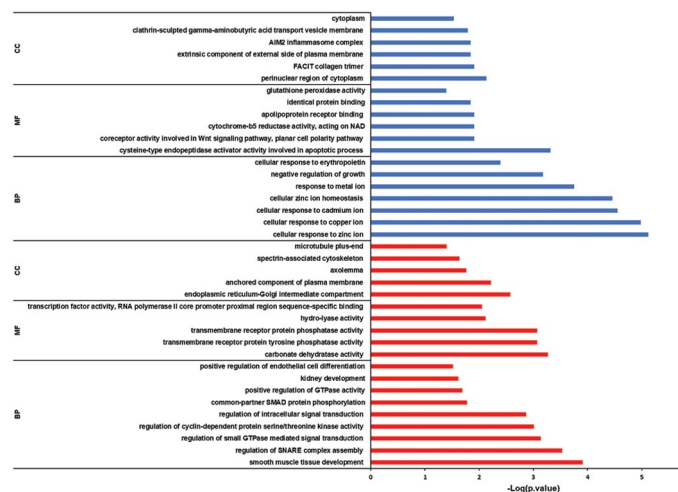


Fig.2: Detecting related gene ontologies. Red and blue columns represent downregulated and upregulated associated GO, respectively. BP; Biological process, MF; Molecular function, and CC; Cellular component.

Further screening of biological processes, separately in the three data series, revealed an increased rate of the cell cycle and inhibition of apoptosis during tumor progression. In addition, epithelial cells loss of differentiation was observed in the group 6, which seems to contribute to the epithelial-to-mesenchymal transition (EMT) that eventually leads to metastasis. EMT promoter genes were also observed in the GOR (Table S4, See Supplementary Online Information at www.celljournal.org). Next, pathway enrichment analysis was accomplished and indicated Nitrogen metabolism and Mineral absorption in the KEGG. Also, erythrocytes take up oxygen and release carbon dioxide and response to metal ions in the Reactome, Suppression of HMGB1 mediated inflammation by the THBD and Zinc homeostasis in the Wikipathways and Oxygen/carbon dioxide exchange in the erythrocytes and Tap63 pathway in the BioPlanet, were detected as the most disrupted pathways for downregulated and upregulated DEGs respectively (Fig.3A).

Disclosing Hub proteins

To identify key proteins with regulatory impacts, the STRING was used for the PPI network construction, and Cytoscape was used for further analysis, which showed that among all common DEGs, 47 proteins were involved in the network via 37 edges (Fig.3B). Considering the degree and betweenness centrality for the nodes indicated BMP4, NQO1, RHOJ, ZNRD1, and GPX4 as the critical proteins (Table S5, See Supplementary Online Information at www.celljournal.org). Analyzing the network with the CentiScape2.2 and CytoHubba plugins demonstrated BMP4 as the most important protein in this PPI network, which is downregulated in group 1 (Fig.S1, See Supplementary Online Information at www.celljournal.org).

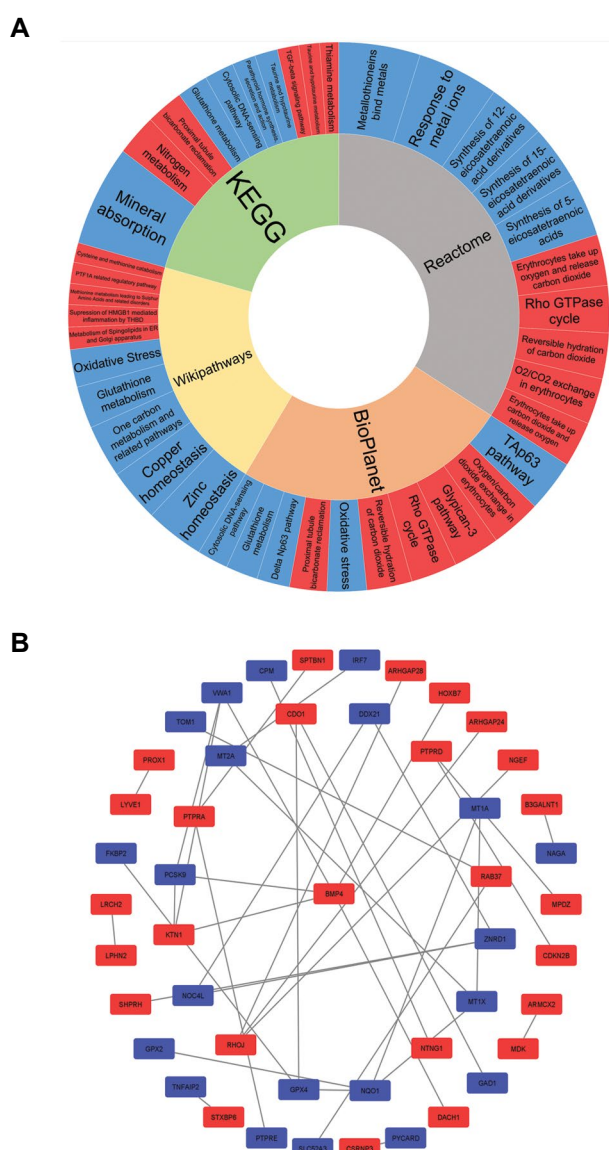


Fig.3: Pathway and network analysis. **A.** Pathway enrichment analysis. Red and blue cells represent downregulated and upregulated pathways, respectively. The most important pathways are those that have bigger cells. **B.** Protein-protein interaction (PPI) network. Red and blue points represent downregulated and upregulated genes.

Accelerate cell cycle and apoptosis arresting during lung adenocarcinoma progression

It seems that the downregulation of *BMP4* during primary tumor progression to stage IB avoids the induction of apoptosis and arresting cell cycle through TGF- β signaling that is needed for tumor progression. Also, the upregulation of *GPX2* through final tumor progression to stage IV (Table S3, See Supplementary Online Information at www.celljournal.org) is correlated with the glutathione metabolism pathway, which maintains the redox balance in the cancer cells against accumulative reactive oxygen species (ROS) and seems to promote EMT, which leads to metastasis. We also found *GPX4* in the glutathione metabolism pathway and *CDKN2B* in the TGF- β signaling that change these pathways in the same way with *BMP4* and *GPX2*. Additionally, screening previous studies on the *GPX2* showed a co-expression relation with *ABCB6* which is involved in the glucose uptake (Fig. S2, See Supplementary Online Information at www.celljournal.org). Hence, upregulation of *GPX2* could result in an increase in the glucose uptake (Fig.4).

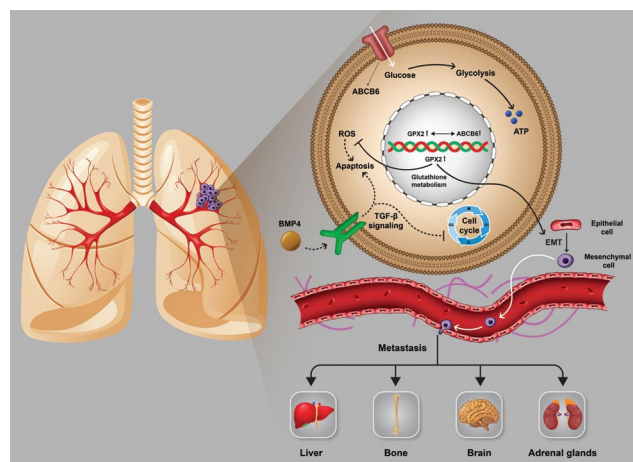


Fig.4: The role of *BMP4* in TGF- β signaling and *GPX2* in glutathione metabolism in tumor progression.

Verification of *GPX2* and *BMP4* in GEPIA database

Screening the expression changes of *BMP4* according to the normal lung tissue in the TCGA data indicated a significant downregulation in the LUSC and non-significant downregulation in the LUAD by $|\text{LogFC}| \geq 1$ and $P < 0.01$ as the cut-off criteria. Analyzing the TCGA data for the *GPX2* showed upregulation in the LUAD and LUSC in comparison with the normal lung tissue (Fig.5A). Monitoring expression alterations of *BMP4* and *GPX2* in the TCGA samples in each stage manifested the same results of GEO and confirmed that *BMP4* was downregulated within a

primary tumor progression to stage IB and *GPX2* was upregulated throughout stage IIB to IV progression (Fig.5B). Kaplan-Mayer analysis illustrated a relation between the downregulation of *BMP4* and upregulation of *GPX2* and the high-risk groups of LUAD patients by considering *GAPDH* as the normalizer gene. Patients with downregulation of *BMP4* approximately between 50-165th month seem to have a lower chance of survival. Contrastingly, upregulation of *BMP4* was correlated with the lower survival rate after 165th. Moreover, upregulation of *GPX2* during the final development of the tumor is related to the high-risk group of patients among approximately 85th month until the 165th month. However, after this period, there was no meaningful difference between the survival chances of LUAD patients, according to the *GPX2* expression (Fig.5C). This information has a predictive potentiality to estimate the life-expectancy of LUAD patients by monitoring their *BMP4* and *GPX2* expression.

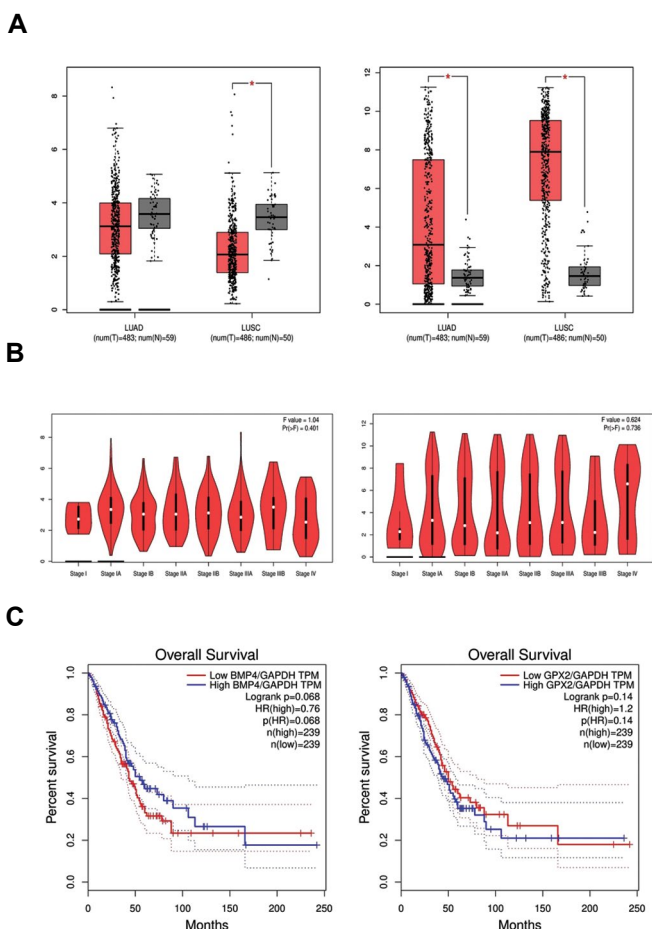


Fig.5: GEPIA analysis of candidate genes. Boxplot of **A.** *BMP4* (left) and *GPX2* (right) in lung adenocarcinoma and lung squamous cell carcinoma. **B.** Stage plot of *BMP4* (left) and *GPX2* (right) in lung adenocarcinoma. **C.** Kaplan-Mayer plotting for survival analysis, divide patients into two groups: high risk and low risk according to *BMP4* downregulation (low TPM) (left) and *GPX2* upregulation (high TPM) (right) by recruiting *GAPDH* as the normalizer gene. TPM; Transcription per million.

Discussion

Lung cancer is described as the most common cancer in both women and men worldwide (18), which leads to the death of 84% of patients (2, 4). Among the mentioned subtypes of this cancer, NSCLC adenocarcinoma is the most diagnosed type of lung cancer (19). Recently, molecular alterations have been suggested as a significant factor to be considered for the cancer treatment instead of other invasive therapeutic methods. Hence, identification of molecular alterations in the NSCLC ADC could suggest candidate genes for treatment and diagnosis that is aimed in the present research. Microarray data in GEO provide a platform for analyzing gene expressions useful for considering molecular changes in cancers (20). In the present study, we have analyzed GSE41272, GSE42127, and GSE75037 (based on GPL6884) in 6 groups, and then common DEGs were identified by Venn in each group. Group 1 (stage IA vs. IB) had the highest number of DEGs suggesting that the molecular reprogramming in the LUAD mostly takes place in the early tumorigenesis. Next, pathway enrichment analysis was performed and showed that upregulated DEGs were enriched in mineral absorption, response to metal ions, zinc homeostasis and TAp63 pathway and downregulated DEGs were enriched in nitrogen metabolism, erythrocytes take up oxygen and release carbon dioxide, suppression of HMGB1 mediated inflammation by THBD and Oxygen/carbon dioxide exchange in erythrocytes using KEGG, Reactome, Wikipathways and BioPlanet databases respectively. Considering involved genes in these pathways suggested that the homeostasis of the metal ions and the metabolism of oxygen and carbon dioxide were important pathways for the NSCLC ADC tumor development. This result is consistent with the observation of carbonate dehydratase activity and cellular response to zinc ion for downregulated and upregulated DEGs via GO analysis by DAVID and Enrichr. By analyzing the biological process in three data series separately, we observed promoted cell proliferation and inhibited apoptosis in all stages of NSCLC ADC, which is in agreement with the tumor progression. Also, the undifferentiation of epithelial cells was observed in the final tumor development to stage IV, which seems to contribute to EMT and distant metastasis.

Subsequently, analyzing of the PPI network by CentiScape2.2 indicated *BMP4* as the critical gene in NSCLC ADC tumor development. According to the GEO and TCGA, *BMP4* was downregulated during cancer progression to the stage IB. *BMP4* has been identified that can act as a tumor suppressor in many cancers through its anti-proliferative, growth inhibitory, metastasis suppressive, and apoptosis-inducing capability (21). Similarly, research on lung cancer demonstrated overexpression of *BMP4* leads to premature senescence of cancerous cells via the Smad signaling pathway by inducing *BMP4* expression with adriamycin (22). In agreement with this, Wen et al. reported that *BMP4* was suppressed in the NSCLC squamous cell carcinoma. It occurs via Sox2 protein that promotes the SCC cell proliferation (21), which is intriguingly consistent with our results.

BMP4 protein is a member of the TGF- β superfamily that has been reported as both tumor suppressor and tumor promoter pathways. In the early stages, TGF- β has been proven to have tumor suppressor activity via cell cycle arrest and inducing apoptosis (23) that is consistent with the Panther and DAVID results for BP. Thus, the downregulation of BMP4 in the TGF- β signaling pathway seems to be essential for primary cancer progressing to the stage IB, which suggests a tumor suppressor activity of BMP4 in the early stages of NSCLC ADC.

Conversely, Mihajlović et al. (24) indicated a pro-migratory and pro-EMT activity for the BMP4 in the NSCLC within BMP receptor type I SMAD dependent signaling by screening LCLC-103H cells, which is compatible with the tumor promoter activity of TGF- β signaling in the final stages (23).

We also observed *GPX2* as the most upregulated gene (Log FC=6.6). A previous study has suggested *GPX2* as an oncogene due to its capability of inducing tumor initiation, growth, development, and metastasis (25). Besides, *GPX2* overexpression was observed in the breast (26), liver (27), gastric (28), nasopharyngeal (29), and esophageal SCC (30). Although, some other studies have reported a positive correlation between *GPX2* expression and cell proliferation in the colorectal cancer and castration-resistant prostate cancer (31, 32) reduced expression of *GPX2* was associated with advanced tumor status in the patients with urothelial carcinomas of the upper urinary tract and urinary bladder (33). Furthermore, Li et al. (34) showed that *GPX2* expression leads to the *MMP2* and *MMP9* expression via activating the Wnt pathway, which subsequently induces epithelial transition to mesenchymal, metastasis, and tumor invasion in the pancreatic tumor, that is interestingly consistent with the upregulation of *GPX2* during stage IIIB to IV progression, which was attained in our results. A previous study by Naiki-Ito et al. (26) reported that *GPX2* played an important role in the mammary carcinogenesis, including humans and rodents. Furthermore, Huang et al. (35) observed that suppression of *GPX2* via YAP pathway relieves lung SCC development. Despite that, a study of the NSCLC cell lines reported that the downregulation of *GPX2* is necessary for EMT induction (36). Moreno Leon et al. (37) found that *GPX2* overexpression increases glucose uptake due to its correlated expression with ABCB6, which was confirmed by GEPIA, suggesting that *GPX2* may modulate the metabolic alteration in the LUAD. Evaluated glucose uptake is required for cancer cell metabolism by providing energy via high rated glycolysis (38, 39).

GPX2, which belongs to the family of glutathione peroxidases, is involved in the maintenance of the redox balance in cells, and it can fulfill its function by protecting cancerous cells against ROS that increases in the tumor microenvironment and damages various macromolecules and induces apoptosis, which was approved via Panther (32, 40). ROS reduction is operated via oxidation of

glutathione by glutathione peroxidases in the glutathione metabolism pathway (40), which was also observed in our KEGG results. In addition, in previous research, the glutathione metabolism pathway has been implicated to induce EMT in the NSCLC (36) that is compatible with our GO analysis in the Panther and DAVID. Therefore, *GPX2*, in the final stages of NSCLC ADC, may be considered to be an oncogene due to its role in providing excessive glucose for tumor cells and glutathione metabolism pathway by inducing EMT and inhibiting apoptosis.

Conclusion

By the integration of 3 microarrays with bioinformatics analysis, we suggested *BMP4* as a tumor suppressor via inducing apoptosis and arresting cell cycle in the early stages, and *GPX2* as an oncogene by inhibiting apoptosis and promoting EMT in advanced stages. They were the two crucial dysregulated genes in the course of tumor development in experimental design, *in vitro* and *in vivo*, to explore the role of these altered genes and to employ them for therapeutic approaches.

Acknowledgments

We appreciate our colleagues for their helpful effort and valuable comments on this research. The authors confirm that methods were performed in accordance with relevant guidelines and regulations. This research did not receive any specific grant from funding agencies in the public, commercial, or not-for-profit sectors. The authors have declared that they have no conflict of interest.

Authors' Contributions

M.H.D.N., A.E.S., A.B.; Designed the project. S.T., A.E.S.; Project supervisor. M.H.D.N., R.A.D., P.Gh.T.; Bioinformatics data analyzer and manuscript writers. A.B., A.A.M., M.H.N., H.M., A.R.; Helper in cancer biology, lung cancer pathology and molecular biology aspects of the research respectively. A.R.; Edits the main text grammatically and revised it. All authors read and approved the final manuscript.

References

1. Torre LA, Siegel RL, Jemal A. Lung cancer statistics. *Adv Exp Med Biol.* 2016; 893: 1-19.
2. Bray F, Ferlay J, Soerjomataram I, Siegel RL, Torre LA, Jemal A. Global cancer statistics 2018: GLOBOCAN estimates of incidence and mortality worldwide for 36 cancers in 185 countries. *CA Cancer J Clin.* 2018; 68(6): 394-424.
3. Collins LG, Haines C, Perkel R, Enck RE. Lung cancer: diagnosis and management. *Am Fam Physician.* 2007; 75(1): 56-63.
4. Nasim F, Sabath BF, Eapen GA. Lung cancer. *Med Clin North Am.* 2019; 103(3): 463-473.
5. Molina JR, Yang P, Cassivi SD, Schild SE, Adjei AA. Non-small cell lung cancer: epidemiology, risk factors, treatment, and survivorship. *Mayo Clin Proc.* 2008; 83(5): 584-594.
6. Ginsberg MS, Grewal RK, Heelan RT. Lung cancer. *Radiol Clin North Am.* 2007; 45(1): 21-43.
7. de Groot P, Munden RF. Lung cancer epidemiology, risk factors, and prevention. *Radiol Clin North Am.* 2012; 50(5): 863-876.
8. Rodriguez-Canales J, Parra-Cuentas E, Wistuba II. Diagnosis and molecular classification of lung cancer. *Cancer Treat Res.* 2016; 170: 25-46.

9. Zheng M. Classification and pathology of lung cancer. *Surg Oncol Clin N Am*. 2016; 25(3): 447-468.
10. Tsim S, O'Dowd CA, Milroy R, Davidson S. Staging of non-small cell lung cancer (NSCLC): a review. *Respir Med*. 2010; 104(12): 1767-1774.
11. Dettterbeck FC, Boffa DJ, Tanoue LT. The new lung cancer staging system. *Chest*. 2009; 136(1): 260-271.
12. Woodard GA, Jones KD, Jablons DM. Lung cancer staging and prognosis. *Cancer Treat Res*. 2016; 170: 47-75.
13. Dachs GU, Dougherty GJ, Stratford IJ, Chaplin DJ. Targeting gene therapy to cancer: a review. *Oncol Res*. 1997; 9(6-7): 313-325.
14. Garnis C, Buys TP, Lam WL. Genetic alteration and gene expression modulation during cancer progression. *Mol Cancer*. 2004; 3: 9.
15. Anisimov SV. Application of DNA microarray technology to gerontological studies. *Methods Mol Biol*. 2007; 371: 249-265.
16. Hanai T, Hamada H, Okamoto M. Application of bioinformatics for DNA microarray data to bioscience, bioengineering and medical fields. *J Biosci Bioeng*. 2006; 101(5): 377-384.
17. Szklarczyk D, Gable AL, Lyon D, Junge A, Wyder S, Huerta-Cepas J, et al. STRING v11: protein-protein association networks with increased coverage, supporting functional discovery in genome-wide experimental datasets. *Nucleic Acids Res*. 2019; 47(D1): D607-D613.
18. Romaszko AM, Doboszyńska A. Multiple primary lung cancer: a literature review. *Adv Clin Exp Med*. 2018; 27(5): 725-730.
19. Cersosimo RJ. Lung cancer: a review. *Am J Health Syst Pharm*. 2002; 59(7): 611-642.
20. Virtanen C, Woodgett J. Clinical uses of microarrays in cancer research. *Methods Mol Med*. 2008; 141: 87-113.
21. Fang WT, Fan CC, Li SM, Jang TH, Lin HP, Shih NY, et al. Down-regulation of a putative tumor suppressor BMP4 by SOX2 promotes growth of lung squamous cell carcinoma. *Int J Cancer*. 2014; 135(4): 809-819.
22. Su D, Zhu S, Han X, Feng Y, Huang H, Ren G, et al. BMP4-Smad signaling pathway mediates adriamycin-induced premature senescence in lung cancer cells. *J Biol Chem*. 2009; 284(18): 12153-12164.
23. Colak S, Ten Dijke P. Targeting TGF- β signaling in cancer. *Trends Cancer*. 2017; 3(1): 56-71.
24. Mihajlović J, Diehl LAM, Hochhaus A, Clement JH. Inhibition of bone morphogenetic protein signaling reduces viability, growth and migratory potential of non-small cell lung carcinoma cells. *J Cancer Res Clin Oncol*. 2019; 145(11): 2675-2687.
25. Du H, Chen B, Jiao NL, Liu YH, Sun SY, Zhang YW. Elevated glutathione peroxidase 2 expression promotes cisplatin resistance in lung adenocarcinoma. *Oxid Med Cell Longev*. 2020; 2020: 7370157.
26. Naiki-Ito A, Asamoto M, Hokaiwado N, Takahashi S, Yamashita H, Tsuda H, et al. Gpx2 is an overexpressed gene in rat breast cancers induced by three different chemical carcinogens. *Cancer Res*. 2007; 67(23): 11353-11358.
27. Liu D, Sun L, Tong J, Chen X, Li H, Zhang Q. Prognostic significance of glutathione peroxidase 2 in gastric carcinoma. *Tumour Biol*. 2017; 39(6): 1010428317701443.
28. Liu T, Kan XF, Ma C, Chen LL, Cheng TT, Zou ZW, et al. GPX2 overexpression indicates poor prognosis in patients with hepatocellular carcinoma. *Tumour Biol*. 2017; 39(6): 1010428317700410.
29. Liu C, He X, Wu X, Wang Z, Zuo W, Hu G. Clinicopathological and prognostic significance of GPx2 protein expression in nasopharyngeal carcinoma. *Cancer Biomark*. 2017; 19(3): 335-340.
30. Lei Z, Tian D, Zhang C, Zhao S, Su M. Clinicopathological and prognostic significance of GPX2 protein expression in esophageal squamous cell carcinoma. *BMC Cancer*. 2016; 16: 410.
31. Emmink BL, Laoukili J, Kipp AP, Koster J, Govaert KM, Fatrai S, et al. GPx2 suppression of H2O2 stress links the formation of differentiated tumor mass to metastatic capacity in colorectal cancer. *Cancer Res*. 2014; 74(22): 6717-6730.
32. Naiki T, Naiki-Ito A, Asamoto M, Kawai N, Tozawa K, Etani T, et al. GPX2 overexpression is involved in cell proliferation and prognosis of castration-resistant prostate cancer. *Carcinogenesis*. 2014; 35(9): 1962-1967.
33. Chang IW, Lin VC, Hung CH, Wang HP, Lin YY, Wu WJ, et al. GPX2 underexpression indicates poor prognosis in patients with urothelial carcinomas of the upper urinary tract and urinary bladder. *World J Urol*. 2015; 33(11): 1777-1789.
34. Li F, Dai L, Niu J. GPX2 silencing relieves epithelial-mesenchymal transition, invasion, and metastasis in pancreatic cancer by down-regulating Wnt pathway. *J Cell Physiol*. 2020; 235(11): 7780-7790.
35. Huang H, Zhang W, Pan Y, Gao Y, Deng L, Li F, et al. YAP suppresses lung squamous cell carcinoma progression via deregulation of the DNP63-GPX2 axis and ROS accumulation. *Cancer Res*. 2017; 77(21): 5769-5781.
36. Matadamas-Guzman M, Zazueta C, Rojas E, Resendis-Antonio O. Analysis of epithelial-mesenchymal transition metabolism identifies possible cancer biomarkers useful in diverse genetic backgrounds. *Front Oncol*. 2020; 10: 1309.
37. Moreno Leon L, Gautier M, Allan R, Ilić M, Nottet N, Pons N, et al. The nuclear hypoxia-regulated NLUCAT1 long non-coding RNA contributes to an aggressive phenotype in lung adenocarcinoma through regulation of oxidative stress. *Oncogene*. 2019; 38(46): 7146-7165.
38. Vanhove K, Graulus GJ, Mesotten L, Thomeer M, Derveaux E, Nobben JP, et al. The metabolic landscape of lung cancer: new insights in a disturbed glucose metabolism. *Front Oncol*. 2019; 9: 1215.
39. Wang Y, Xia Y, Lu Z. Metabolic features of cancer cells. *Cancer Commun (Lond)*. 2018; 38(1): 65.
40. Bansal A, Simon MC. Glutathione metabolism in cancer progression and treatment resistance. *J Cell Biol*. 2018; 217(7): 2291-2298.